



## Preparation, Characterization and Stability of Li-ion Conducting $\text{Li}_{1.5}\text{Al}_{0.5}\text{Ge}_{1.5}(\text{PO}_4)_3$ Glass-Ceramic with NASICON-Type Structure

Mahdi Kazazi<sup>\*a</sup>, Mohammad Illbeigi<sup>b</sup>, Alireza Fazlali<sup>b</sup>, Amir. H. Mohammadi<sup>c,d,e</sup>

<sup>a</sup> Department of Materials Engineering, Faculty of Engineering, Malayer University, P.O. Box 65719-95863, Malayer, Iran

<sup>b</sup> Department of Chemical Engineering, Faculty of Engineering, Arak University, Arak, Iran

<sup>c</sup> Institut de Recherche en Génie Chimique et Pétrolier (IRGCP), Paris Cedex, France

<sup>d</sup> Thermodynamics Research Unit, School of Engineering, University of KwaZulu-Natal, Howard College Campus, King George V Avenue, Durban 4041, South Africa

<sup>e</sup> Département de Génie des Mines, de la Métallurgie et des Matériaux, Faculté des Sciences et de Génie, Université Laval, Québec (QC), G1V 0A6, Canada

### PAPER INFO

#### Paper history:

Received 29 December 2015

Accepted in revised form 18 June 2016

#### Keywords:

NASICON-type glass ceramic,  
Lithium-air battery,  
 $\text{LiNO}_3$  electrolyte, Stability

### ABSTRACT

A super ionic conducting lithium aluminum germanium phosphate (LAGP) glass-ceramic with a formula of  $\text{Li}_{1.5}\text{Al}_{0.5}\text{Ge}_{1.5}(\text{PO}_4)_3$  was synthesized by melt-quenching method and subsequent crystallization at 850 °C for 8 h. The prepared glass-ceramic was characterized using differential scanning calorimetry (DSC), X-ray diffraction (XRD), field emission scanning electron microscopy (FESEM), and AC impedance techniques. The XRD patterns exhibited the existence of  $\text{LiGe}_2(\text{PO}_4)_3$  as the dominant phase with a little impurity phase of  $\text{GeO}_2$ . SEM images revealed the presence of large LAGP crystals. A high conductivity of  $5.36 \times 10^{-3}$  S/cm at 25 °C was obtained for the pristine LAGP glass-ceramic. Furthermore, the stability of the LAGP was examined in 1 M  $\text{LiNO}_3$  aqueous solution by XRD and conductivity measurements. XRD pattern and ionic conductivities of the immersed LAGP show no changes compare to the pristine LAGP and indicate the high ionic conductivity and good stability in  $\text{LiNO}_3$  aqueous electrolyte and these two properties are essential for lithium-protective layer in aqueous lithium-air batteries.

## 1. INTRODUCTION

With rapid growth of various portable applications, especially electric vehicles (EVs) and hybrid electric vehicles (HEVs), it is necessary to develop rechargeable batteries with high energy and power density, and high safety [1–3]. Rechargeable lithium ion batteries are of great interest due to their high volumetric and gravimetric energy density [4]. However, to drive an electric vehicle for long distances, the energy density of conventional Li-ion batteries is insufficient [5]. Moreover, these types of batteries usually use liquid organic electrolytes, which are flammable and volatile. Hence, these electrolytes are not appropriate for transportation industry due to the explosion probability during high-rate charge or discharge [6]. These problems have restricted the utilization of conventional lithium batteries in electric vehicles.

Lithium-air batteries have attracted a lot of attentions over the past years because of their high theoretical energy density which is higher than that of the conventional lithium ion batteries [7]. These batteries have great potentials to meet the electric vehicle needs

[8–11]. All Li-air battery systems employ lithium metal as the anode and oxygen gas, supplied from outside of the battery, as the cathode material. Two types of lithium-air batteries have been developed; aqueous and non-aqueous systems. The non-aqueous system has higher energy density than the aqueous system, but it has some serious problems, including high polarization for the charge and discharge processes, electrolyte decomposition, and electrolyte contamination by moisture from the cathode side [12, 13]. The replacement of organic electrolyte with the aqueous electrolyte is an effective way to solve these problems [14]. In spite of the advantages of aqueous electrolytes, metallic lithium anode reacts severely with water and should be covered with a water-stable lithium conducting solid electrolyte as membrane [15]. This protective layer should have some critical properties, including high lithium ion conducting, aqueous electrolyte stability, stability in contact with lithium metal and impermeability for water molecules and air [14, 16].

Ceramic ionic conductors based on the NASICON-type structure such as  $\text{LiTi}_2(\text{PO}_4)_3$  and  $\text{LiGe}_2(\text{PO}_4)_3$  are promising groups of oxide-based solid lithium-ion conductors [17]. However, in relation to Li ions,  $\text{Ti}^{4+}$

\* Corresponding Author Email: [m\\_kazazi@malayeru.ac.ir](mailto:m_kazazi@malayeru.ac.ir), [mahdi.kazazi@gmail.com](mailto:mahdi.kazazi@gmail.com) (M. Kazazi)

may not be as stable as  $\text{Ge}^{4+}$  [18, 19].  $\text{LiGe}_2(\text{PO}_4)_3$  NASICON-type glass-ceramic were crystallized in 3D network structure (rhombohedral crystal system, space group R3c) which has appropriate channels for Li ions migration. There are two types of polyhedrons,  $\text{GeO}_6$  octahedra and  $\text{PO}_4$  tetrahedra, which are attached by their corners to form  $[\text{Ge}(\text{PO}_4)]$  frame with 3D interconnected channels and two types of interstitial cavities,  $A_1$  and  $A_2$ . Li ions migrate in channels of this frame. Li ions can occupy in  $A_1$  and  $A_2$  sites. In  $\text{LiGe}_2(\text{PO}_4)_3$  with no dopant,  $A_2$  sites are vacant while  $A_1$  sites are occupied by Li ions [20]. Partial substitution of  $\text{Ge}^{4+}$  ions by trivalent cations such as  $\text{Al}^{3+}$  ions increases the unit cell dimensions and residual negative charges are neutralized by additional Li ions. Changing in unit cell dimensions and Li ion concentration in crystal leads to increment in ionic conductivity [20, 21].

One of the major issues facing aqueous lithium-air batteries is protection of metallic lithium anode against aqueous electrolytes. In the present study, NASICON-type  $\text{Li}_{1.5}\text{Al}_{0.5}\text{Ge}_{1.5}(\text{PO}_4)_3$  (LAGP) glass-ceramic was prepared by melt-quenching method and its microstructure and ionic conductivity were investigated. In addition, the stability of the LAGP glass-ceramic immersed in  $\text{LiNO}_3$  aqueous electrolyte was examined by XRD and AC impedance measurements. The obtained results show that the prepared LAGP glass-ceramic has high ionic conductivity and good stability in  $\text{LiNO}_3$  aqueous electrolyte, and both properties are essential for lithium-protective layer in aqueous lithium-air batteries.

## 2. EXPERIMENTAL

### 2.1. LAGP Glass-Ceramic Preparation

The melt-quenching method was used to prepare the LAGP glass-ceramic. Stoichiometric amounts of germanium dioxide ( $\text{GeO}_2$ , 99.8%, Merck, 112177), lithium carbonate ( $\text{Li}_2\text{CO}_3$ , 99.9%, Merck, 105680), aluminum oxide ( $\text{Al}_2\text{O}_3$ , 99.5%, Sigma-Aldrich, 265497) and ammonium dihydrogen phosphate ( $\text{NH}_4\text{H}_2\text{PO}_4$ , 99.5%, Merck, 101126) were used as the starting materials to prepare  $\text{Li}_{1.5}\text{Al}_{0.5}\text{Ge}_{1.5}(\text{PO}_4)_3$  glass-ceramic. Powders were weighed with an accuracy of 0.0001 g and mixed for 20 min in an agate mortar and pestle. Then they were heated in electrical furnace at 700 °C for 2 h in order to decompose ammonia, carbon dioxide and water vapor out from the starting materials. Finally, the puff shape materials were crushed in agate mortar and pestle and were transformed in a platinum crucible and heated in electrical furnace at 1450 °C for 1 h. The homogeneous melted glass was pressed and quenched between two preheated (300 °C) stainless steel plates. The transparent thin glass sheets were transferred to another furnace and were annealed at 550 °C for 2 h to release the thermal stresses and then cooled down to room temperature. To obtain the glass-ceramic specimens, annealed glass

sheets were crystallized at 850 °C for 8 h with a heating rate of 5 °C/min.

### 2.2. Characterization and Stability Examination

Thermal behavior of the glass (glass transition temperature ( $T_g$ ) and crystallization temperature ( $T_c$ )) was analyzed by Differential Scanning Calorimetry (DSC, NETZSCH 404 F1 Pegasus-High Temperature DSC, Germany) on the fine powdered glass with a heating rate of 5 °C/min. The crystal structure of the specimens was identified by X-ray diffraction analysis (XRD, Xmd300 Unisantis, Germany) at room temperature using  $\text{Cu K}\alpha$  radiation source in  $2\theta$  range from 0 to 60°. The microstructure and energy dispersion spectroscopy (EDS) of the glass-ceramic specimen were obtained with a field emission scanning electron microscope (FESEM, Sigma-vp Zeiss, Germany) on the fractured surfaces.

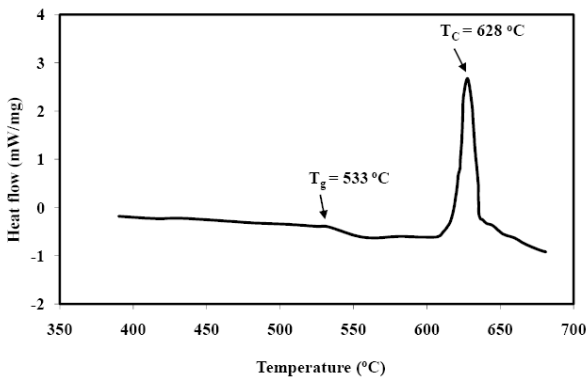
In order to investigate the stability of the LAGP sample, the LAGP plate was immersed in 1 M  $\text{LiNO}_3$  aqueous solution for 1 month. After this time, the sample was washed with water and dried at 200 °C for overnight to remove the residual water content. The changes of XRD patterns and the ionic conductivity after immersion were examined. The ionic conductivity of the crystallized sample before and after immersion test was determined at the temperatures of 20, 26, 30, 40, 50, 60, 70 and 80 °C using impedance spectroscopy analyzer (Metrohm Autolab PGST302, Netherlands) in the frequency range of  $10^{-1}$ - $10^5$  Hz, with the voltage amplitude of  $\pm 100$  mV. Samples for the AC impedance measurement were polished to obtain uniform thickness and flat surfaces. Furthermore, the opposite faces were coated with silver paint for good electrical contact. The impedance data were analyzed using the ZSim program.

## 3. RESULTS AND DISCUSSION

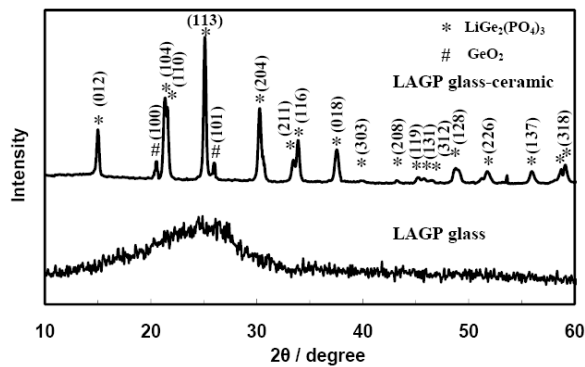
The DSC curve for the non-annealed LAGP glass is shown in Figure 1. The LAGP glass exhibited a distinct and strong exothermic crystallization peak,  $T_c$ , at around 628 °C with a glass transition temperature,  $T_g$ , at around 533 °C. The exothermic peak is attributed to the crystallization temperature,  $T_c$ . The estimated  $T_g$  and  $T_c$  values well match with previously reported values in similar systems [16, 22]. Based on this result, crystallization was performed at a temperature above  $T_c$  for ensuring perfect crystallization.

Figure 2 shows the XRD patterns of the LAGP specimen before and after thermal treatment at 850 °C for 8 h. In the case of LAGP glass-ceramic, the main diffraction peaks are related to the NASICON-type phase of  $\text{LiGe}_2(\text{PO}_4)_3$  (JCPDS card 80-1924). Unlike the extensive substitution of  $\text{Al}^{3+}$  at the  $\text{Ge}^{4+}$  sites, the diffraction patterns match closely and no peaks related to

the  $\text{Al}_2\text{O}_3$  phase are observed. The extensive substitution of  $\text{Al}^{3+}$  for  $\text{Ge}^{4+}$  is attributed to the similar ionic radii of  $\text{Ge}^{4+}$  (0.53 Å) and  $\text{Al}^{3+}$  (0.54 Å) [23, 24]. The LAGP phase is dominant in the glass-ceramic sample, and other peaks indicate the presence of  $\text{GeO}_2$  phase. However, based on this thermal treatment procedure, no impurity  $\text{AlPO}_4$  phase is observed in the XRD pattern of LAGP glass-ceramic. The  $\text{AlPO}_4$  impurity is electrically insulating phase and is expected to decrease the conductivity of the glass-ceramic material, even in smaller concentrations [24].



**Figure 1.** Differential scanning calorimetry plot of as-cast LAGP sample



**Figure 2.** XRD patterns of the LAGP specimen before and after thermal treatment at 850 °C for 8 h

The field emission scanning electron microscopy (FESEM) micrographs of the fractured surfaces of the LAGP glass and glass-ceramic specimens are shown in Figure 3(a) and (b), respectively. In Fig. 3(a), there is no crystal or grain due to the fast cooling of melt. It indicates that a complete amorphous phase was obtained using this synthesis procedure (melt-quenching between two stainless steel sheets). As can be seen, the LAGP glass is very dense and uniform and no pores are observed. It is believed that the existence of the pores in the solid conductive samples decreases the ionic conductivity. The micrograph of the LAGP glass-ceramic shows grown and well-defined crystals and the grains and grain boundaries are completely distinct. The grains are mostly in cubic

shape and the grain size distribution is almost uniform. On the other hand, Figure 4 shows energy-dispersive X-ray spectroscopy (EDS) of the LAGP glass-ceramic. The obtained result from the EDS analysis of the specified area is in good agreement with initial stoichiometry. In general, lithium element cannot be determined by EDS analysis. However, Li has only 2.5 wt% in overall formula of  $\text{Li}_{1.5}\text{Al}_{0.5}\text{Ge}_{1.5}(\text{PO}_4)_3$ , which does not have great effect on analysis of other elements. Table 1 shows the obtained values from the elemental analysis of the specified area on Figure 4.

To apply glass-ceramics in the aqueous lithium-air batteries, it is necessary to check the stability of glass-ceramics in the aqueous electrolytes. Hence, the stability of the prepared LAGP glass-ceramic was evaluated by immersing the LAGP sample in 1 M  $\text{LiNO}_3$  aqueous solution for 1 month at 25 °C. Figure 5 shows the XRD patterns of the LAGP glass-ceramic before and after 1 month immersion test. As shown in this figure, no change in the XRD pattern of the immersed LAGP sample is observed. In fact, no notable decrease in peak intensities or no new diffraction peaks are observed after immersion test. This result indicates that the LAGP glass-ceramic is stable and durable for a long period of time in contact with  $\text{LiNO}_3$  aqueous electrolyte and can be used in the lithium-air batteries with this electrolyte.

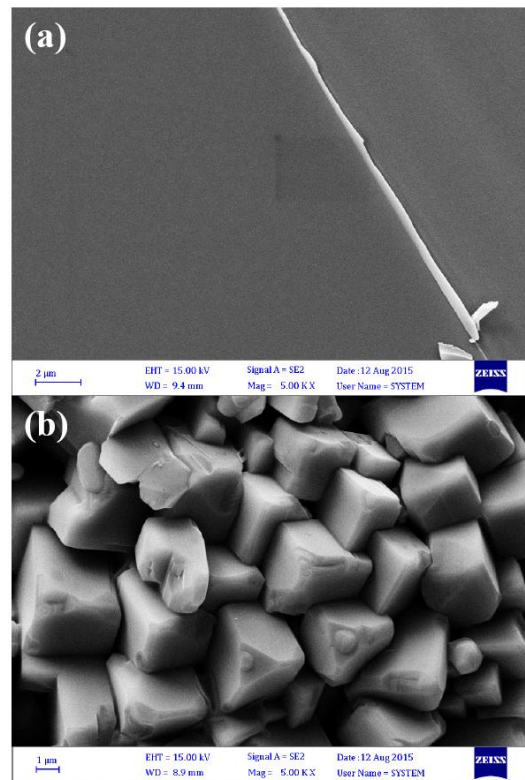


**Figure 3.** FESEM images of the LAGP specimen (a) before and (b) after crystallization

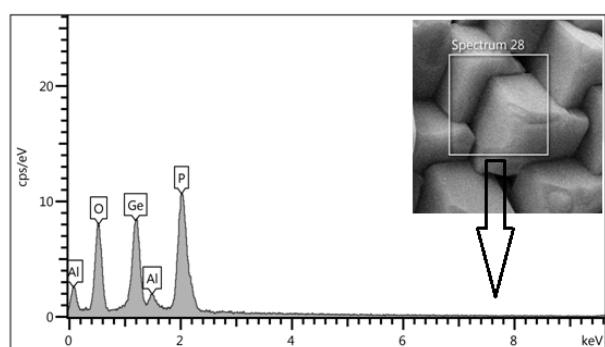


**Figure 4.** Energy-dispersive X-ray spectroscopy (EDS) of the specified area for the prepared LAGP glass-ceramic

**TABLE 1.** Elemental analysis (weight percent) of the specified area in Figure 4

	Al	Ge	P	O	Li
Theoretical values in $\text{Li}_{1.5}\text{Al}_{0.5}\text{Ge}_{1.5}(\text{PO}_4)_3$	3.23	26.08	22.24	45.96	2.49
Measured values	3.1	27.3	22.6	47.0	-

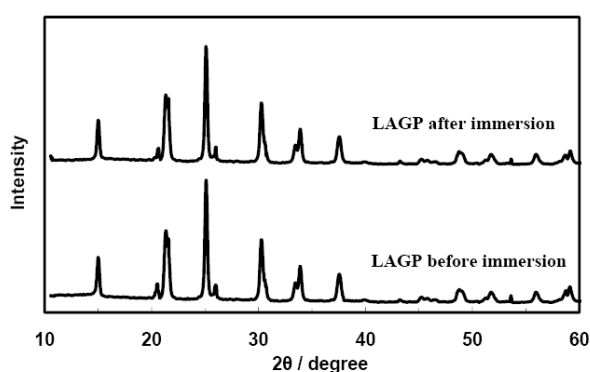


**Figure 5.** XRD patterns of the pristine LAGP and the LAGP immersed for 1 month in 1 M  $\text{LiNO}_3$  aqueous solution

The stability of the LAGP glass-ceramic sample immersed in 1 M  $\text{LiNO}_3$  aqueous solutions was also confirmed from the impedance spectroscopy observations. In fact, the stability of ionic conductivity is a key factor for glass-ceramics for commercial application in the aqueous lithium batteries. In Figure 6, the complex impedance plot of the pristine LAGP sample is compared with those of the LAGP specimen immersed in the 1 M  $\text{LiNO}_3$  aqueous solution at room temperature for 3 days, 1 week and 1 month. All spectra show a semicircle, attributed to the grain boundary resistance of the LAGP glass-ceramic. Indeed, due to the high ionic conductivity of the grains at room temperature, the semicircle related to the grain conductivity cannot be observed. The intercept of the semicircle on the real axis at high-frequency region represents the bulk resistance,

and the straight line in the low-frequency region corresponds to the Warburg impedance (W), which may be attributed to specimen interaction observed for a typical ion conducting solid electrolyte with a blocking electrode [25-27]. In fact, the coarse grains result in decrease in the grain boundaries, lead to enhance lithium ion mobility and hence a higher total conductivity. In order to analyze the obtained EIS spectra, equivalent circuit displayed in Figure 6 was employed. Total ionic conductivity was calculated by following equation [16]:

$$\sigma_t = \frac{d}{S.R_t} \quad (1)$$

Where  $R_t$ ,  $S$  and  $d$  are total resistance (summation of grain and grain boundary resistances), painted area and thickness of specimen, respectively. The ionic conductivities of the LAGP glass-ceramic before and after immersing in various times are summarized in Table 2. As can be seen from Figure 6 and Table 2, no significant change of the impedance profiles is observed for immersion time up to 1 month and only the grain boundary resistance slightly increases. The conductivity of the glass-ceramics depends on the microstructure. Hence, the conductivity stability of the LAGP sample during immersion test shows that no significant change occurs in its microstructural characterization. This result is consistent with the XRD results and both show the stability of the LAGP glass-ceramic with  $\text{LiNO}_3$  aqueous electrolyte.

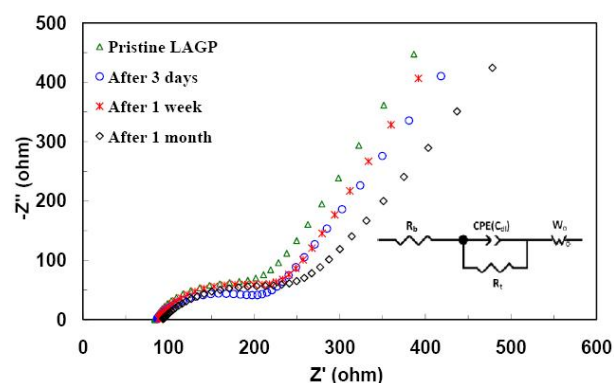


**Figure 6.** Complex impedance plots at room temperature of the LAGP specimen immersed in 1 M  $\text{LiNO}_3$  aqueous solution for various times

**TABLE 2.** Ionic conductivities of the LAGP glass-ceramic before and after immersion in 1 M  $\text{LiNO}_3$  aqueous solution for various times

Immersion time	Ionic conductivity (S/cm)
Before immersion	$5.36 \times 10^{-3}$
3 days	$5.11 \times 10^{-3}$
1 week	$4.82 \times 10^{-3}$
1 month	$4.57 \times 10^{-3}$



The temperature dependence of the total conductivity of the pristine LAGP glass-ceramic and the LAGP sample immersed in 1 M LiNO<sub>3</sub> aqueous solution for 1 month is shown in Figure 7. These conductivities were obtained from the impedance spectroscopy tests performed in the temperature range of 20-80 °C. As can be seen, the plots of log( $\sigma_t$ ) versus 1000/T are found to be linear and well fit the Arrhenius equation taken by following equation [28]:

$$\sigma_t = A \exp\left(\frac{-E_a}{kT}\right) \quad (2)$$

Where A, E<sub>a</sub>, K and T are pre-exponential factor, activation energy, Boltzmann constant and absolute temperature, respectively. The consistent of the plots with the Arrhenius equation demonstrates that there were no structure and phase change for both samples in the testing temperature range [3]. It has been shown that if an impurity phase such as AlPO<sub>4</sub> forms at the grain boundaries by increasing the temperature, the conductivity-temperature plots will be nonlinear [5, 16, 17, 29]. The AlPO<sub>4</sub> phase is a dielectric and has a blocking effect that prevents from easy migration of lithium ions. However, linearity of the obtained plots shows the stability of the prepared LAGP glass-ceramic against elevated temperatures. As a result, the activation energy of the prepared LAGP glass-ceramic was measured to be 0.286 eV. Moreover, it can be seen from this figure that total electrical conductivity of the LAGP sample is the same both before and after immersion, and indicates the stability of the LAGP sample in contact with LiNO<sub>3</sub> aqueous electrolyte.

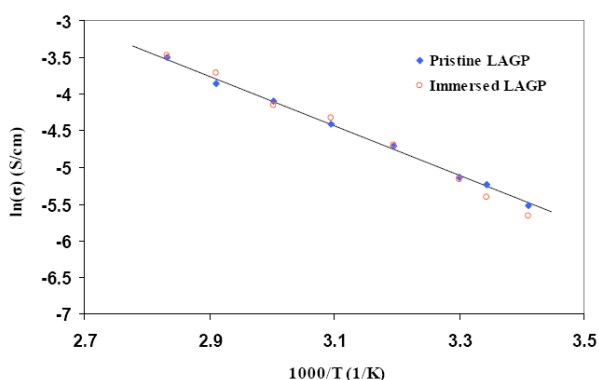


**Figure 7.** Temperature dependence of ionic conductivity of the LAGP specimen before and after 1 month immersion in 1 M LiNO<sub>3</sub> aqueous solution

#### 4. CONCLUSION

A NASICON-type glass ceramic with a formula of Li<sub>1.5</sub>Al<sub>0.5</sub>Ge<sub>1.5</sub>(PO<sub>4</sub>)<sub>3</sub> as fast lithium ion conductor was synthesized by melt-quenching method and subsequent crystallization. The prepared glass-ceramic was characterized by DSC, XRD and FESEM

and its ionic conductivity was examined by impedance spectroscopy. Then, the stability of the LAGP sample in 1 M LiNO<sub>3</sub> aqueous solution was examined. XRD patterns of the LAGP immersed in the solution at room temperature for 1 month show no changes. Also, no significant conductivity change was observed during immersion test. The above results show the stability of the LAGP glass-ceramic in contact with this aqueous electrolyte, which is very important for practical application in the aqueous lithium-air batteries or other lithium batteries with aqueous electrolytes.

#### ACKNOWLEDGMENTS

This work was financially supported by Malayer University.

#### REFERENCE

- Xu X.X., Wen Z.Y., Gu Z.H., Lin Z.X., "High lithium conductivity in Li<sub>1.3</sub>Cr<sub>0.3</sub>Ge<sub>1.7</sub>(PO<sub>4</sub>)<sub>3</sub> glass-ceramics", *Materials Letters*, Vol. 58, (2004), 3428–3431.
- Kazazi M., "Synthesis and elevated temperature performance of a polypyrrole-sulfur-multi-walled carbon nanotube composite cathode for lithium sulfur batteries", *Ionics*, Vol. 22, (2016), 1103-1112.
- Xu X., Wen Z., Gu Z., Xu X., Lin Z., "Preparation and characterization of lithium ion-conducting glass-ceramics in the Li<sub>1+x</sub>Cr<sub>x</sub>Ge<sub>2-x</sub>(PO<sub>4</sub>)<sub>3</sub> system", *Electrochemistry Communications*, Vol. 6, (2004), 1233–1237.
- Tarascon J.M., Armand M., "Review article issues and challenges facing rechargeable lithium batteries", *Nature*, Vol. 414, (2001), 359-367.
- Kazazi M., Ghadami F., Dadfar M.R., Sobhani M., Mohammadi A.H., "Effect of synthesis method on the morphological and electrochemical characteristics of sulfur/MWCNT composite cathode", *Solid State Ionics*, Vol. 290, (2016), 40-46.
- Goodenough J.B., Kim Y., "Challenges for rechargeable Li batteries", *Chemistry of Materials*, Vol. 22, (2009), 587-603.
- Mariappan C.R., Gellert M., Yada C., Rosciano F., Roling B., "Grain boundary resistance of fast lithium ion conductors: Comparison between a lithium-ion conductive Li-Al-Ti-P-O-type glass ceramic and a Li<sub>1.5</sub>Al<sub>0.5</sub>Ge<sub>1.5</sub>P<sub>3</sub>O<sub>12</sub> ceramic", *Electrochemistry Communications*, Vol. 14, (2012), 25-28.
- Bruce P.G., Freunberger S.A., Hardwick L.J., Tarascon J.M., "Li-O<sub>2</sub> and Li-S batteries with high energy storage", *Nature Materials*, Vol. 11, (2012), 19-29.
- Armand M., Tarascon J.M., "Building better batteries", *Nature*, Vol. 451, (2008), 652-657.
- Irishkumar G., McCloskey B., Luntz A.C., Swanson S., Wilcke W., "Lithium-air battery: Promise and challenges", *Journal of Physical Chemistry Letters*, Vol. 1, (2010), 2193-2203.
- Kraytsberg A., Ein-Eli Y., "Review on lithium-air batteries- Opportunities, limitations and perspective", *Journal of Power Sources*, Vol. 196, (2011), 886-893.
- Hasegawa S., Imanishi N., Zhang T., Xie J., Hirano A., Takeda Y., Yamamoto O., "Study on lithium/air secondary batteries—Stability of NASICON-type lithium ion conducting glass-ceramics with water", *Journal of Power Sources*, Vol. 189, (2009), 371–377.

13. Kuboki T., Okuyama T., Ohsaki T., Takami N., "Lithium-air batteries using hydrophobic room temperature ionic liquid electrolyte", *Journal of Power Sources*, Vol. 146, (2005), 766–769.
14. Zhang M., Takahashi K., Uechi I., Takeda Y., Yamamoto O., Im D., Lee D.J., Chi B., Pu J., Li J., Imanishi N., "Water-stable lithium anode with  $\text{Li}_{1.4}\text{Al}_{0.4}\text{Ge}_{1.6}(\text{PO}_4)_3\text{-TiO}_2$  sheet prepared by tape casting method for lithium-air batteries", *Journal of Power Sources*, Vol. 235, (2013), 117-121.
15. He K., Zu C., Wang Y., Han B., Yin X., Zhao H., Liu Y., Chen J., "Stability of lithium ion conductor NASICON structure glass ceramic in acid and alkaline aqueous solution", *Solid State Ionics*, Vol. 254, (2014), 78-81.
16. Thokchom J.S., Kumar B., "Composite effect in superionically conducting lithium aluminium germanium phosphate based glass-ceramic", *Journal of Power Sources*, Vol. 185, (2008), 480-485.
17. Thokchom J.S., Gupta N., Kumar B., "Superionic conductivity in a lithium aluminum germanium phosphate glass-ceramic", *Journal of The Electrochemical Society*, Vol. 155, (2008), A915-A920.
18. Fu J., "Superionic conductivity of glass-ceramic in the system  $\text{Li}_2\text{O-Al}_2\text{O}_3\text{-TiO}_2\text{-P}_2\text{O}_5$ ", *Solid State Ionics*, Vol. 96, (1997), 195-200.
19. Xu X., Wen Z., Gu Z., Xu X., Lin Z., "Lithium ion conductive glass ceramics in the system  $\text{Li}_{1.4}\text{Al}_{0.4}(\text{Ge}_{1-x}\text{Ti}_x)_{1.6}(\text{PO}_4)_3$  ( $x = 0-1.0$ )", *Solid State Ionics*, Vol. 171, (2004), 207–213.
20. Sun Y., "Lithium ion conducting membranes for lithium-air batteries", *Nano Energy*, Vol. 2, (2013), 801–816.
21. Chowdari B.V.R., Rao G.V.S., Lee G.Y.H., "XPS and ionic conductivity studies on  $\text{Li}_2\text{O-Al}_2\text{O}_3\text{-(TiO}_2\text{ or GeO}_2\text{)-P}_2\text{O}_5$  glass-ceramics", *Solid State Ionics*, Vol. 136, (2000), 1067–1075.
22. Fu J., "fast  $\text{Li}^+$  ion conducting in the system  $\text{Li}_2\text{O-Al}_2\text{O}_3\text{-GeO}_2\text{-P}_2\text{O}_5$ ", *Solid State Ionics*, Vol. 104, (1997), 191-194.
23. Thokchom J.S., Kumar B., "The effects of crystallization parameters on the ionic conductivity of a lithium aluminum germanium phosphate glass-ceramic", *Journal of Power Sources*, Vol. 195, (2010), 2870–2876.
24. Kumar B., Thomas D., Kumar J., "Space-charge-mediated superionic transport in lithium ion conducting glass-ceramics", *Journal of The Electrochemical Society*, Vol. 156, (2009), A506-A513.
25. Bruce P.G., West A.R., "The A-C conductivity of polycrystalline LISICON,  $\text{Li}_{2+2x}\text{Zn}_{1-x}\text{GeO}_4$ , and a model for intergranular constriction resistances", *Journal of The Electrochemical Society*, Vol. 130, (1983), 652-669.
26. Yao X.L., Xie S., Nian H.Q., Chen C.H., "Spinel  $\text{Li}_4\text{Ti}_5\text{O}_{12}$  as a reversible anode material down to 0 V", *Journal of Alloys and Compounds*, Vol. 465, (2008), 375–379.
27. Xu X., Wen Z., Wu X., Yang X., Gu Z., "Lithium ion-conducting glass-ceramics of  $\text{Li}_{1.5}\text{Al}_{0.5}\text{Ge}_{1.5}(\text{PO}_4)_{3-x}\text{Li}_2\text{O}$  ( $x=0.05-0.20$ ) with good electrical and electrochemical properties", *Journal of American Ceramic Society*, Vol. 90, (2007), 2802-2806.
28. Zhang M., Huang Z., Cheng J., Yamamoto O., Imanishi N., Chi B., Pu J., Li J., "Solid state lithium ionic conducting thin film  $\text{Li}_{1.4}\text{Al}_{0.4}\text{Ge}_{1.6}(\text{PO}_4)_3$  prepared by tape casting", *Journal of Alloys and Compounds*, Vol. 590, (2014), 147–152.
29. Shim onishi Y., Zhang T., Johnson P., Imanishi N., Hirano A., Takeda Y., Yamamoto O., Sammes N., "A study on lithium/air secondary batteries-Stability of NASICON-type glass ceramics in acid solutions", *Journal of Power Sources*, Vol. 195, (2010), 6187-6191.